Calibration of a Measuring Robot: Experimental Results on a 5 DOF Structure

Alberto Omodei, Giovanni Legnani,*
Riccardo Adamini
Dip. Ingegneria Meccanica
Università di Brescia
Via Branze 38
25123 Brescia, Italy
e-mail: legnani@bsing.ing.unibs.it

Received 6 November 1999; accepted 2 January 2001

An original method for the static calibration of robots using the pose matching approach is presented. Three algorithms for the identification of the structural parameters are investigated. The procedure includes a methodology to automatically remove the unnecessary parameters for the robot under analysis. After a theoretical introduction, the methodology is practically applied to an actual 5 DOF measuring robot used in a shoe manufactory industry. The accuracy of the robot is increased up to its repeatability.

1. INTRODUCTION

Generally industrial robots have a high repeatability (up to few 1/100 mm), but their accuracy is worse (up to some millimeters). Where a higher accuracy is required, robots are programmed in teaching mode: the end effector is moved manually to some desired poses, the corresponding joint rotations are recorded, and these values are utilized to reposition the robot when necessary. Accuracy becomes important when we wish to program robots using pre-determined knowledge about their tasks. We could calculate the joint displacement required for a robot in advance, knowing the kinematic arrangement of its mechanism.[1,2]

In many application the effect of load deformation is low and the main source of pose error is geometrical inaccuracy. Robots are made with care, but many small errors in the mechanical structure contribute to form pose errors. Geometrical inaccuracy means that some structural parameters are slightly different from their nominal value. If the motion of the robot is planned using the nominal geometry, gripper position errors are generated. If

*To whom all correspondence should be addressed.
Contract grant sponsor: MURST grant ex40% ''Progetto METAFORE.''

the actual value of the structural parameters can be identified, the robot accuracy can be improved greatly.

The calibration process usually reduces the pose errors from several millimeters to a few tenths of millimeters or less. In practical cases the accuracy that can be reached through calibration is close to the repeatability of the robot.

Measuring robots have similar problems. A measuring robot is an open kinematic structure with angular position detectors measuring the joint angle rotations (generally incremental encoders are used). If the robot end effector is driven to a certain pose, this one can be estimated by the measures performed by the encoders and knowing the robot kinematics. Errors in the robot kinematics produce inaccuracy in the pose estimation.

The aim of this article is the development and the comparison between different methodologies for the identification of the structural parameters of a measuring robot currently used in shoe manufacturing industries. The calibration procedure must be used by nonskilled operators in production environment, must be fast and reliable, and must not require decisions by the operator. After a theoretical introduction, results of practical experimentation are given.

2. CALIBRATION BASES

The purpose of a kinematic model of a robot is to relate the joint displacements with the pose of the end effector. This model will contain a set of coefficients that describes the geometry of a particular robot. Calibration is the process of determining the set of parameters in the model that best describes the specific robot under study. Calibration can be performed by two different approaches: *pose measuring*[3] and *pose matching*.[4]

Using the pose measuring approach the robot is requested to reach a predefined "*desired*" pose $\mathbf{S}_d$ and the calibration process is performed elaborating the difference between $\mathbf{S}_d$ and the "*actual*" pose $\mathbf{S}_a$ reached by the gripper.

In this article we use the *pose matching* approach. The robot gripper is driven to a number of known poses and the corresponding joint rotations are measured. The difference between the expected joint coordinates and the actual ones is used as input for the identification procedure. For a given robot, the joint coordinates $\mathbf{Q}$ are related to the gripper pose $\mathbf{S}$ by the direct kinematics $F(\cdot)$ and its inverse $G(\cdot)$:

$$\begin{aligned} \mathbf{S} &= F(\mathbf{Q}, \mathbf{L}) \qquad & \mathbf{Q} &= [\, q_1, q_2, \ldots, q_i, \ldots, q_n \,]^T \\ \mathbf{Q} &= G(\mathbf{S}, \mathbf{L}) \qquad & \mathbf{L} &= [\, l_1, l_2, \ldots, l_j, \ldots, l_m \,]^T \\ & & \mathbf{S} &= [\, s_1, \ldots, s_6 \,]^T \end{aligned} \tag{1}$$

Vector $\mathbf{L}$ includes the geometric parameters of the robot, e.g., the Denavit and Hartenberg parameters (D&H).[5,6]

Linearizing Eq. (1) in the neighborhood of $\mathbf{S} = \mathbf{S}_0$, $\mathbf{Q} = \mathbf{Q}_0$, $\mathbf{L} = \mathbf{L}_0$ with $\mathbf{S}_0 = \mathbf{F}(\mathbf{Q}_0, \mathbf{L}_0)$ we get

$$\mathbf{S} - \mathbf{S}_0 \cong \frac{\partial F}{\partial \mathbf{L}}(\mathbf{L} - \mathbf{L}_0) + \frac{\partial F}{\partial \mathbf{Q}}(\mathbf{Q} - \mathbf{Q}_0) \tag{2}$$

which can be written also as

$$\Delta \mathbf{S} \cong \frac{\partial F}{\partial \mathbf{L}} \Delta \mathbf{L} + \frac{\partial F}{\partial \mathbf{Q}} \Delta \mathbf{Q} \tag{3}$$

Many calibration procedures are based on this linearized equation.

A "good" calibration model must fulfill two criteria: completeness and proportionality.

- A complete and "minimum" model contains a sufficient number of parameters to describe the mechanical structure of a robot without being redundant.
- A parameterization is proportional if discontinuities are not present and small changes in the geometry of the robot are reflected by small changes in the parameters. For example the D&H parameterization[6] fails to be proportional for nearly parallel contiguous joint axes.[5]

Such a good model is referred as CPC (complete, proportional, and continuous).[3,5]

As is well known, when only constant geometrical errors in the structure are considered, indicating with R and P the number of revolute and prismatic DOF, the number of the geometric parameters to be calibrated is[5]

$$m = 6 + 4R + 2P \tag{4}$$

3. IDENTIFYING THE PARAMETER VALUES

3.1. Pose Measuring

If we ask the robot gripper to move to a certain desired pose $\mathbf{S}_d$, the gripper will reach the actual pose $\mathbf{S}_a$:

$$\mathbf{S}_a = F(\mathbf{Q}_d, \mathbf{L}_n + \Delta\mathbf{L}) \qquad \text{with } \mathbf{Q}_d = G(\mathbf{S}_d, \mathbf{L}_n) \quad (5)$$

where $\mathbf{Q}_d$ are the joint rotations evaluated by the inverse kinematic based on the nominal value of the robot parameters $\mathbf{L}_n$, and $\Delta\mathbf{L}$ are the geometrical parameter errors. The error in the gripper pose will be

$$\Delta\mathbf{S} = \mathbf{S}_a - \mathbf{S}_d$$

Assuming that the magnitude of the parameter errors is small, we can linearize the equations as

$$\Delta\mathbf{S} \cong \mathbf{J}_L \cdot \Delta\mathbf{L} \qquad \mathbf{J}_L = \frac{\partial F}{\partial \mathbf{L}} \quad (6)$$

where $\mathbf{J}_L$ is Jacobian matrix evaluated with respect to the geometrical parameters evaluated for $\mathbf{Q} = \mathbf{Q}_d$ and $\mathbf{L} = \mathbf{L}_n$.

Equation (6) gives a scalar equation for each coordinate of the gripper pose that can be measured, six at most.

If the value of $\Delta\mathbf{S}$ can be measured for a sufficient number of poses, it is possible to estimate the value of $\Delta\mathbf{L}$ that minimizes the difference between the measured poses and those predicted by Eq. (5). Three approaches are given in Section 3.4. The required equations are obtained by rewriting Eq. (6) for each pose. A graphical representation of the procedure is presented in Figure 1.

3.2. Pose Matching

When we force the robot gripper to reach a certain desired pose $\mathbf{S}_d$, we predict the joint rotations $\mathbf{Q}_d$ using the inverse kinematic based on the nominal values $\mathbf{L}_n$ of the structural parameters,

$$\mathbf{Q}_d = G(\mathbf{S}_d, \mathbf{L}_n)$$

where $G(\cdot)$ is the inverse kinematics.

However, the actual value joints $\mathbf{Q}_a$ are different from the predicted values because the geometrical parameters are afflicted by errors:

$$\mathbf{Q}_a = G(\mathbf{S}_d, \mathbf{L}_n + \Delta\mathbf{L}) \cong \mathbf{Q}_d + \frac{\partial G}{\partial \mathbf{L}}\Delta\mathbf{L} \quad (7)$$

Also

$$\mathbf{Q}_a - \mathbf{Q}_d \cong \frac{\partial G}{\partial \mathbf{L}}\Delta\mathbf{L} \quad (8)$$

$\Delta\mathbf{L}$ is the vector containing the geometrical parameter errors and $\frac{\partial G}{\partial \mathbf{L}}$ is evaluated for $\mathbf{S} = \mathbf{S}_d$ and $\mathbf{L} = \mathbf{L}_n$. A proper calibration determines the value of $\Delta\mathbf{L}$ that minimizes the difference between the measured joint rotations and those predicted by Eq. (7).

Equation (8) for pose matching is the equivalent of Eq. (6) for pose measuring. Since $\frac{\partial G}{\partial \mathbf{L}}$ is generally not available, an alternative formulation can be used.

Linearizing the direct kinematics equation we have

$$\mathbf{S}_a \cong F(\mathbf{Q}_d, \mathbf{L}_n) + \frac{\partial F}{\partial \mathbf{L}}\Delta\mathbf{L} + \frac{\partial F}{\partial \mathbf{Q}}(\mathbf{Q}_a - \mathbf{Q}_d) \quad (9)$$

Since $\mathbf{S}_a$ has been forced to be equal to $F(\mathbf{Q}_d, \mathbf{L}_n)$, we get

$$\frac{\partial F}{\partial \mathbf{L}}\Delta\mathbf{L} + \frac{\partial F}{\partial \mathbf{Q}}\Delta\mathbf{Q} \cong 0 \qquad \Delta\mathbf{Q} = \mathbf{Q}_a - \mathbf{Q}_d$$

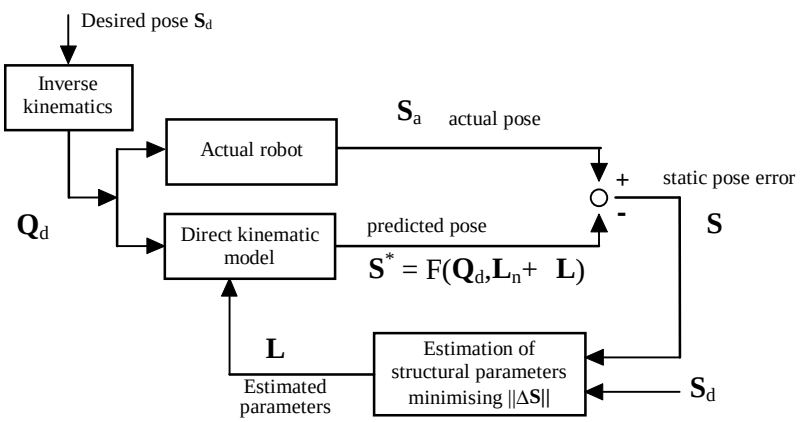

Figure 1. Calibration of a robot using the pose measuring approach.

and so

$$\frac{\partial F}{\partial \mathbf{L}}\Delta\mathbf{L} \cong -\frac{\partial F}{\partial \mathbf{Q}}\Delta\mathbf{Q} \tag{10}$$

Equation (10) is equivalent to Eq. (8) but does not require the knowledge of $\frac{\partial G}{\partial \mathbf{L}}$.

The number of the geometrical parameters m to be estimated is greater than the number of the joint rotations that can be measured for each gripper pose. However, if the value of $\Delta\mathbf{Q}$ can be measured for a sufficient number of poses, it is possible to estimate the value of $\Delta\mathbf{L}$. Three estimation procedures are given in Section 3.4. The required equations are obtained rewriting by Eq. (10) for all the poses. A graphical representation of the procedure is given in Figure 2.

3.3. Equivalence between Pose Matching and Pose Measuring

Equivalence between pose matching and pose measuring can be established remembering that for a given value of the structural parameters we have

$$\Delta\mathbf{S} \cong \frac{\partial F}{\partial \mathbf{Q}}\Delta\mathbf{Q}$$

As already stated in Section 3.1 the pose measuring approach for calibration is based on the difference between the predicted and the measured poses corresponding to the same joint rotations. The same procedure can be used any time that a set of a corresponding pair of joint rotation $\mathbf{Q}_a$ and gripper pose $\mathbf{S}_a$ is known for the actual robot.

In Section 3.1 we forced the joint coordinates to known values and we measured the corresponding gripper pose. The alternative approach of Section 3.2 consists of forcing a known gripper pose and measuring the corresponding joint rotations.

Moreover, calibration procedures written for the pose measuring approach can be used also for the pose matching case using the following guidelines.

The robot gripper is forced to a known pose $\mathbf{S}_a$. The actual joint coordinates $\mathbf{Q}_a$ are measured. The theoretical gripper position $\mathbf{S}^*$ is predicted using the direct kinematic for $\mathbf{Q} = \mathbf{Q}_a$. Then the robot calibration for pose measuring is performed using $\mathbf{Q}_a$ for $\mathbf{Q}_d$, $\mathbf{S}^*$ for $\mathbf{S}_d$. If the correct value of $\Delta\mathbf{L}$ is identified we get $\mathbf{S}^* = \mathbf{S}_a$. A graphical representation of the resulting algorithm for pose matching is presented in Figure 3.

This is the procedure used for the experimentation described in Section 5.

3.4. Estimation of Structural Parameters

3.4.1. Calibration Procedure

For the estimation of the structural parameters, three different identification procedures based on the guidelines presented in Section 3.3 have been realized and compared:

1. a nonlinear optimization procedure;
2. an iterative linearization of the equations;
3. an extended *Kalman* filter.

The robot is driven to a set of known poses $\mathbf{S}_{ah}$ $(h = 1, 2, \ldots, k)$ using the dime described in Section 4.1 and the corresponding joint rotation $\mathbf{Q}_{ah}$ is recorded. The mathematical procedures described in Sections 3.4.2, 3.4.3, and 3.4.4 are then applied to estimate the structural parameters.

3.4.2. Nonlinear Optimization Procedure ("Amoeba")

The first method, experimented by the authors to estimate the geometrical parameter errors, consists of writing Eq. (5) for a sufficient number of poses

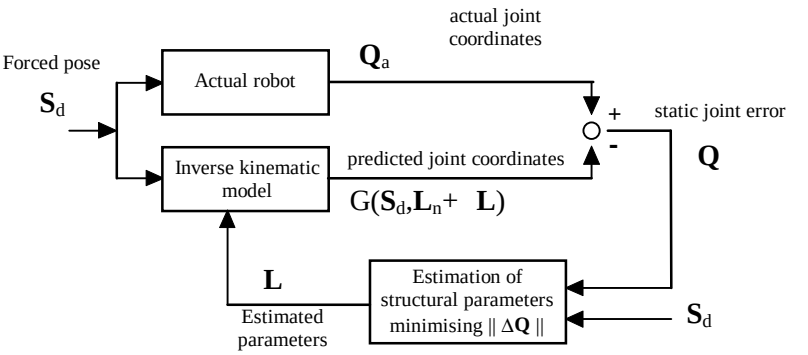

Figure 2. Calibration of a robot using the pose matching method.

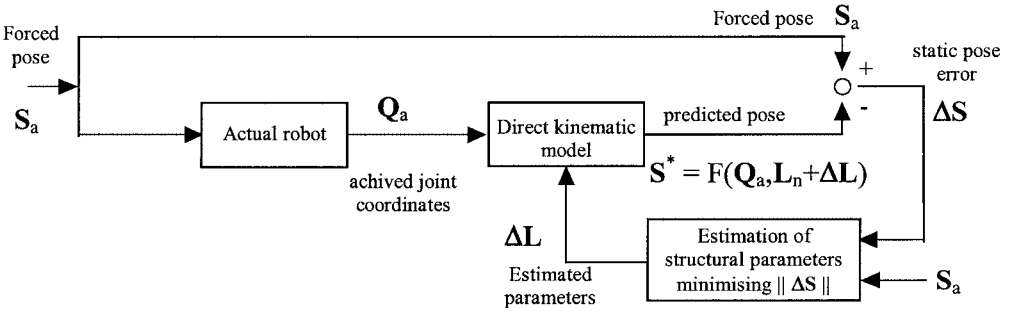

Figure 3. Scheme of the estimation algorithm used (pose matching).

and using a general purpose optimization algorithm to find the value of $\Delta\mathbf{L}$ which minimizes the average error E_{op} based on the Euclidean norm:[3,11]

$$E_{\text{op}} = \frac{1}{k}\sum_{h=1}^{k} \|\mathbf{S}_{ah} - F(\mathbf{Q}_{ah}, \mathbf{L}_n + \Delta\mathbf{L})\| \qquad (11)$$

E_{op} is also called the residual. The subscript h is used to scan the k measured poses, $\mathbf{S}_{ah}$ is the hth imposed gripper pose, and $F(\cdot)$ is the predicted value for $\mathbf{S}$. In the theoretical error free case, if the value of $\Delta\mathbf{L}$ is exactly evaluated, E_{op} would be exactly null. A series of $\mathbf{S}_{ah}$ and $\mathbf{Q}_{ah}$ must be given to the algorithm that working on the whole set, after several iterations, gives an estimation of the value of $\Delta\mathbf{L}$ which minimizes E_{op}.

The optimization procedure we adopted is call *amoeba* and it is adapted from ref. 7.

3.4.3. Iterative Linearization of the Equations ("Linear")

The second method experimented consists of writing Eq. (6) for a sufficient number of poses and grouping all the equations in a linear system that can be solved to find $\Delta\mathbf{L}$:[3,11]

$$\mathbf{A}\cdot\Delta\mathbf{L} = \mathbf{b} \qquad \mathbf{A} = \begin{bmatrix} \mathbf{A}_1 \\ \vdots \\ \mathbf{A}_h \\ \vdots \\ \mathbf{A}_k \end{bmatrix} \qquad \mathbf{b} = \begin{bmatrix} \mathbf{b}_1 \\ \vdots \\ \mathbf{b}_h \\ \vdots \\ \mathbf{b}_k \end{bmatrix} \qquad (12)$$

where $\mathbf{A}_h$ is $\mathbf{J}_L$ evaluated for the hth pose and $\mathbf{b}_h = \Delta\mathbf{S}_h = \mathbf{S}_{ah} - F(\mathbf{Q}_{ah}, \mathbf{L}_n)$.

The measures are generally redundant and so the system is solved with the least squares criteria. Solving the linear system Eq. (12) gives a first estimation of the structural parameter errors. Using Eq. (12) recursively improves the accuracy of the result.[3,11] At each iteration j the last value of the parameters $\mathbf{L}_{j+1}$ replaces $\mathbf{L}_j$:

$$\mathbf{L}_{j+1} = \mathbf{L}_j + \Delta\mathbf{L}_j \qquad \text{with } \mathbf{L}_0 = \mathbf{L}_n \qquad (13)$$

This procedure is repeated iteratively until the average error E_{it} reaches a stable minimum:

$$E_{\text{it}} = \frac{1}{k}\sqrt{\mathbf{b}^T\mathbf{b}} \qquad (14)$$

E_{it} is also called residual and is consistent with Eq. (11).

3.4.4. An Extended Kalman Filter ("Kalman")

A *Kalman* filter is a mathematical procedure to estimate the state of a system when uncertainties are present. Assuming that the vector of the geometrical parameters $\Delta\mathbf{L}$ represents the state of a stationary system, an extended *Kalman* filter can be defined to give an estimation of $\Delta\mathbf{L}$ starting from $\Delta\mathbf{S}$.[4,8] In these circumstances, the algorithm is often referred to as "recursive least squares" estimation.[3,11]

The filter gives a new estimation of $\Delta\mathbf{L}$ each time a new measure of $\Delta\mathbf{S}$ is considered. The estimation $\Delta\mathbf{L}_{h+1}$ of $\Delta\mathbf{L}$, after the hth pose has been imposed, is

$$\Delta\mathbf{L}_{h+1} = \Delta\mathbf{L}_h + \mathbf{M}_h(\mathbf{S}_{ah} - F(\mathbf{Q}_{ah}, \mathbf{L}_n + \Delta\mathbf{L}_h))$$

$$\mathbf{M}_h = \mathbf{P}_h\mathbf{C}_h^T(\mathbf{R} + \mathbf{C}_h\mathbf{P}_h\mathbf{C}_h^T)^{-1} \qquad \Delta\mathbf{L}_0 = 0$$

$$\mathbf{P}_{h+1} = (\mathbf{1} - \mathbf{M}_h\mathbf{C}_h)\mathbf{P}_h$$

where $\mathbf{C}_h$ is the Jacobian $\mathbf{J}_L$ evaluated in the hth pose, $\mathbf{M}_h$ is the filter matrix gain after h steps, and $\mathbf{P}_h$ is the matrix of the parameters covariance. $\mathbf{R}$ is the matrix of the measures covariance. $\mathbf{P}_0$ representing the initial uncertainty of $\mathbf{L}$ should be initialized with suitable large values. The diagonal value of $\mathbf{P}$ contains a prediction of the accuracy of the estimation of $\Delta\mathbf{L}$, while $\mathbf{R}$ contains an estimation of the noise present in the measuring procedure.

Non-null extra diagonal elements in position i, j of matrices $\mathbf{P}$ (or $\mathbf{R}$) indicate that the ith and jth parameters (or the ith and the jth measures) are correlated.

$\mathbf{R}$ and a series of $\mathbf{S}_{ah}$ and $\mathbf{Q}_{ah}$ must be given to the algorithm, which estimates $\Delta\mathbf{L}$ and $\mathbf{P}$.

A correct choice of $\mathbf{R}$ and $\mathbf{P}_0$ is essential for a good convergence of the algorithm. The values must be chosen depending on the expected error of the actual robot and of the measuring devices. Values must be adjusted using simulations.

After the processing of all the poses, an index error E_{ka} can be evaluated using Eq. (11).

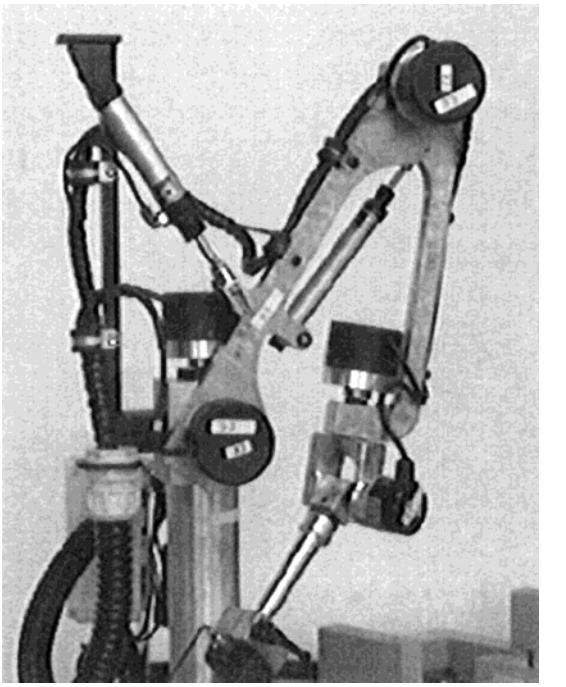

Figure 4. Structure of the 5 DOF measuring robot.

4. ACTUAL SYSTEM

4.1. Measuring Robot

Figure 4 shows the measuring robot whose kinematics structure is better described in Section 4.3. The measuring robot employed in a shoe industry is used to manually measure the shape of the shoe soles by touching them with the robot end effector. The robot is requested to measure the position of the distal point of the end effector and the direction of its axis. For this reason the structure has five rotational DOF. Equation (4) would suggest the identification of 26 parameters for a complete calibration. However, in our case the end effector rotation around its axis has no importance and cannot be measured in the actual robot; then only a total of $m = 25$ structural parameters must be identified.

The joint displacements are measured by high resolution encoders with a resolution of 0.018 degrees for step, which gives a theoretical gripper repeatability of about ± 0.17 mm.

The robot is made by steel, the structure is quite stiff, its weight is partially compensated by compressed air pistons, and it is not subjected to loads during operation. High precision incremental encoders are directly connected to the revolute joints. For these reasons a pure kinematics calibration was considered appropriate.

4.2. Dime for Pose Matching

To force the robot gripper to a sufficient number of different poses, a precision dime was constructed (see Figure 5). The holes in the dime are intended for the intersection of the pin attached on the robot gripper (Figure 6). The holes were created on different surfaces of the dime. The dime fills most of the working space where the robot must work.

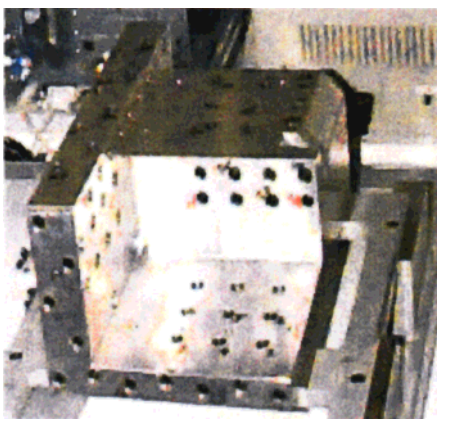

Figure 5. Dime. [Color figure can be viewed in the online issue, which is available at www.interscience.wiley.com.]

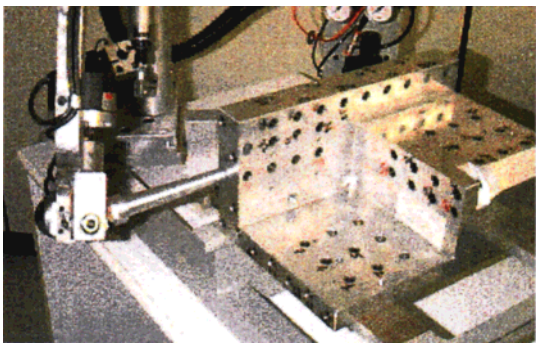

Figure 6. Matching a robot pose using the dime. [Color figure can be viewed in the online issue, which is available at www.interscience.wiley.com.]

The dime was made by a numeric control tool machine, the position and orientation of each hole was measured by a tri-dimensional measure machine, and temperature was compensated with a precision of one micron (DEA model SWIFT A0.00 MOT). Each hole is represented by its axis and the point obtained by the intersection of the hole axis with the plane representing the dime surface. During the calibration procedure the operator inserts the gripper pin into the holes and collects the joint angles. These values are recorded together with the correspondent theoretic gripper pose.

In our case, the robot has 25 parameters; for each pose we can measure the joint coordinates (5 data) and so we must repeat the measurement for a minimum of $25/5 = 5$ poses.[8,9] However, to improve the calibration accuracy and to cover the useful part of the working area with different gripper orientations the measuring dime was designed to have 46 insertion holes. Some of them can be reached with two different robot configurations. For this reason we can force the robot to a total of 81 different configuration obtaining 81 independent measures.

4.3. Parameters of the Robot to be Estimated

The 5 DOF robot under analysis has a structure similar to that of a PUMA robot. The direct kinematic problem was solved using a D&H procedure. An inverse kinematic solution was also derived in analytical form for $\mathbf{L} = \mathbf{L}_n$.

Figure 7 shows a schematic view of the 5 DOF robot. Frame {0} is embedded on the robot base, while frames from {1} to {5} are embedded on the corresponding link using the D&H convention[6] (axis z_i coincident with joint axis $i + 1$).

The absolute reference frame {G} is the frame with respect to which every measurement is taken. In the theoretical error free case {G} is located on the robot base with the z axis parallel to first joint axis and is coincident with frame {0}. z_0 is not parallel to z_G but its nonparallelism is caused by very small constant rotations $\delta\chi_0$ and $\delta\psi_0$ around x_G and y_G. The theoretical position of frame {0} with respect to {G} is $[X_0, Y_0, 0]^T$ and two position errors ΔX_0 and ΔY_0 are identified. Translations in the z direction are incorporated in the length of link 1.

The pose of frame {0} with respect to {G} is then represented by $\mathbf{M}_{G0}$:

$$\mathbf{M}_{G0} = \mathrm{Trans}(x_0, X_0 + \Delta X_0) \cdot \mathrm{Trans}(y_0, Y_0 + \Delta Y_0) \cdot \mathrm{Rot}(x_0, \chi_0 + \delta\chi_0) \cdot \mathrm{Rot}(y_0, \psi_0 + \delta\psi_0)$$

$$\mathbf{M}_{G0} = \begin{bmatrix} c_\psi & 0 & s_\psi & X \\ s_\chi \cdot s_\psi & c_\chi & -s_\chi \cdot c_\psi & Y \\ -c_\chi \cdot s_\psi & s_\chi & c_\chi \cdot c_\psi & 0 \\ 0 & 0 & 0 & 1 \end{bmatrix} \quad \begin{aligned} \chi &= \chi_0 + \delta\chi_0 \\ \psi &= \psi_0 + \delta\psi_0 \\ X &= X_0 + \Delta X_0 \\ Y &= Y_0 + \Delta Y_0 \end{aligned} \tag{15}$$

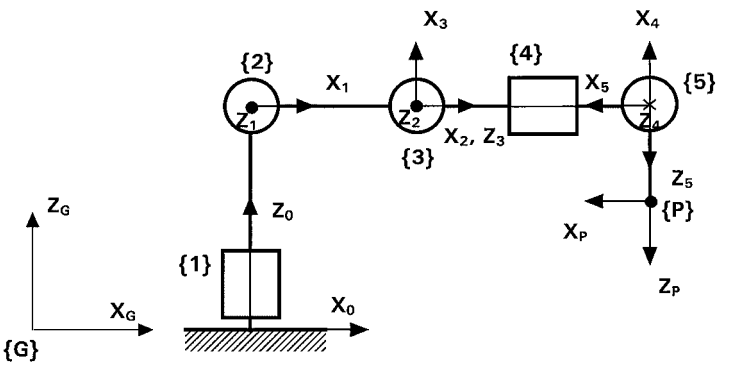

Figure 7. Frame positions.

where each parameter is the sum of its nominal value plus its error. A lowercase δ marks the increments of angular coordinates, while an uppercase Δ marks those of linear terms. Moreover, the sine and the cosine of angles are abbreviated as follows:

$$c_a = \cos(\alpha)$$
$$s_a = \text{sen}(\alpha)$$

According to the D&H convention, the matrix representing the relative position between frame $i-1$ and i is

$$\begin{aligned}\mathbf{M}_{i-1,i} = &\text{Rot}(z_{i-1}, \vartheta_i + \delta\vartheta_i + q_i)\\ &\cdot\text{Trans}(z_{i-1}, d_i + \Delta d_i)\\ &\cdot\text{Trans}(x_i, a_i + \Delta a_i)\cdot\text{Rot}(x_i, \alpha_i + \delta\alpha_i)\end{aligned} \tag{16}$$

where each parameter ϑ_i, d_i, a_i, and α_i is the sum of its nominal value plus its error and q_i is the ith joint coordinate. With the exception of $\mathbf{M}_{12}$ we get

$$\mathbf{M}_{i-1,j} = \begin{bmatrix} c_\vartheta & -s_\vartheta\cdot c_\alpha & s_\vartheta\cdot s_\alpha & a\cdot c_\vartheta \\ s_\vartheta & c_\vartheta\cdot c_\alpha & -c_\vartheta\cdot s_\alpha & a\cdot s_\vartheta \\ 0 & s_\alpha & c_\alpha & d \\ 0 & 0 & 0 & 1 \end{bmatrix} \quad \begin{aligned}\vartheta &= \vartheta_i + \delta\vartheta_i + q_i\\ \alpha &= \alpha_i + \delta\alpha_i\\ a &= a_i + \Delta a_i\\ d &= d_i + \Delta d_i\\ i &= 1,3,4,5\end{aligned} \tag{17}$$

Since joint axes 2 and 3 are parallel, in order to avoid singularities in the calibration procedures, the transformation between frame {1} and {2} should be expressed in term of a suitable set of structural parameters.[5] A suitable formulation for $\mathbf{M}_{12}$ is

$$\begin{aligned}\mathbf{M}_{12} = &\text{Rot}(z_1, \vartheta_2 + \delta\vartheta_2 + q_2)\cdot\text{Trans}(z_1, d_2)\\ &\cdot\text{Trans}(x_2, a_2 + \Delta a_2)\cdot\text{Rot}(x_2, \alpha_2 + \delta\alpha_2)\\ &\cdot\text{Rot}(y_2, \psi_2 + \delta\psi_2)\end{aligned}$$

We get

$$\mathbf{M}_{12} = \begin{bmatrix} c_\vartheta\cdot c_\psi - s_\vartheta\cdot s_\alpha\cdot s_\psi & -s_\vartheta\cdot c_\alpha & c_\vartheta\cdot s_\psi + s_\vartheta\cdot s_\alpha\cdot c_\psi & a\cdot c_\vartheta \\ s_\vartheta\cdot c_\psi + c_\vartheta\cdot s_\alpha\cdot s_\psi & c_\vartheta\cdot c_\alpha & s_\vartheta\cdot s_\psi - c_\vartheta\cdot s_\alpha\cdot c_\psi & a\cdot s_\vartheta \\ -c_\alpha\cdot s_\psi & s_\alpha & c_\alpha\cdot c_\psi & d \\ 0 & 0 & 0 & 1 \end{bmatrix} \quad \begin{aligned}\vartheta &= \vartheta_2 + \delta\vartheta_2 + q_2\\ \alpha &= \alpha_2 + \delta\alpha_2\\ a &= a_2 + \Delta a_2\\ d &= d_2 = 0\\ \psi &= \psi_2 + \delta\psi_2\end{aligned} \tag{18}$$

Two frames are embedded on the last link (''the gripper'') and two matrices are necessary to describe its geometry ($\mathbf{M}_{45}$ and $\mathbf{M}_{5P}$) with a total of four constant parameters plus the rotation of the last joint. The frames are {5} and {P}. Their relative position is

$$\mathbf{M}_{5P} = \begin{bmatrix} 1 & 0 & 0 & 0 \\ 0 & 1 & 0 & 0 \\ 0 & 0 & 1 & Z_P + \Delta Z_P \\ 0 & 0 & 0 & 1 \end{bmatrix}$$

The absolute gripper pose is represented by a product of the position matrices:

$$\mathbf{M}_{GP} = \mathbf{M}_{G0}\cdot\prod_{i=1}^{5}\mathbf{M}_{i-1,i}\cdot\mathbf{M}_{5P}$$

The joint coordinates q_i are included in the joint vector $\mathbf{Q}$, while the joint offsets ϑ_i are contained in vector $\mathbf{L}$.

Therefore the joint coordinates are

$$\mathbf{Q} = [\,q_1 \quad q_2 \quad q_3 \quad q_4 \quad q_5\,]^T$$

and the complete set of the structural parameters is

$$\begin{aligned}\mathbf{L} = [\,&X_0 \quad Y_0 \quad \chi_0 \quad \psi_0 \quad \vartheta_1 \quad d_1 \quad a_1 \quad \alpha_1 \quad \vartheta_2 \quad a_2\\ &\alpha_2 \quad \psi_2 \quad \vartheta_3 \quad d_3 \quad a_3 \quad \alpha_3 \quad \vartheta_4 \quad d_4 \quad a_4 \quad \alpha_4\\ &\vartheta_5 \quad d_5 \quad a_5 \quad \alpha_5 \quad Z_p\,]^T\end{aligned}$$

and their nominal values are

$$\begin{aligned}\mathbf{L} = [\,&0 \quad 0 \quad 0° \quad 0° \quad (0°) \quad 252 \quad 0 \quad 90° \quad (0°) \quad 320\\ &0 \quad 0° \quad (90°) \quad 0 \quad 0 \quad 90° \quad (0°) \quad 330 \quad 0 \quad 90°\\ &(-90°) \quad 0 \quad 0 \quad 90° \quad 161\,]^T\end{aligned}$$

Lengths are given in millimeters and angles in degrees. Data in parentheses represent the nomi-

nal value of the joint coordinate offsets. For $\mathbf{Q} = [0\ 0\ 0\ 0\ 0]^T$, the robot assumes the configuration of Figure 7.

5. RESULTS AND DISCUSSION

To verify the algorithms, we initially tested them with simulated measures. The simulated data were created as follows. A number of joint rotations $\mathbf{Q}^{\#}$ were chosen and the corresponding gripper poses $\mathbf{S}^{\#}$ were evaluated giving an arbitrary value to the structural parameter errors $\Delta\mathbf{L}^{\#}$. The programs under test were asked to estimate the structural errors $\Delta\mathbf{L}$ assuming $\mathbf{Q}_a = \mathbf{Q}^{\#}$ and $\mathbf{S}_a = \mathbf{S}^{\#}$. In the theoretical case, $\Delta\mathbf{L}$ should as a result be identical to $\Delta\mathbf{L}^{\#}$. Before running the estimation procedure, the joint coordinates and the poses were corrupted, adding random errors to simulate uncertainties in the measuring system. The convergence of the procedure and the achieved accuracy were estimated comparing $\mathbf{S}^{\#}$ with $F(\mathbf{Q}^{\#}, \mathbf{L}_n + \Delta\mathbf{L})$. The results showed that if only geometric inaccuracy is present, it is possible to reach a robot accuracy close to the measuring error. When the noise was set to zero, the parameters were estimated with an error close to the round-off error ($< 10^{-8}$).

The simulation activity was also useful in the design of the dime and in choosing its optimal location. The three estimation algorithms were used in the iterative design, taking advantage by their different characteristics: linear was very fast and useful for multiple runs, *kalman* was precious for the information contained in the covariance matrices, and *amoeba* was useful because it was able to improve the accuracy after calibration to the best values, giving an indication on the top performance that can be expected. The simulation was also useful for the tuning of the value of the covariance matrices $\mathbf{R}$ and $\mathbf{P}_0$ of *kalman*. Both matrices were chosen to be diagonal. The optimal values for the diagonal elements of $\mathbf{R}$ were found to be $(2 \cdot 10^{-5})^2 m^2$ for the terms associated to the gripper position, and $(3 \cdot 10^{-4})^2$ for the term associated with orientation. The diagonal elements of $\mathbf{P}_0$ were all set to $(5 \cdot 10^{-3})^2$.

As a final step, experimental calibration was performed on the actual system (see Figure 8). The measuring robot was forced to reach a set of predefined known poses and, for each of them, the corresponding joint rotations were measured.To estimate the robot repeatability, all the poses were forced twice by two different operators recording the correspondent joint rotations. The gripper positions were evaluated with the nominal value of the parameters and the difference between the two sets was evaluated. The maximum difference was 0.353 mm which gives a distance $d = 0.176$ from the average position. The average distance was $\bar{d} = 0.082$ mm and its standard deviation was $\sigma = 0.062$ mm. Borrowing a definition from international standards,[10] we estimated the robot repeatability as $RP \cong \bar{d} + 3\sigma = \pm 0.268$ mm.

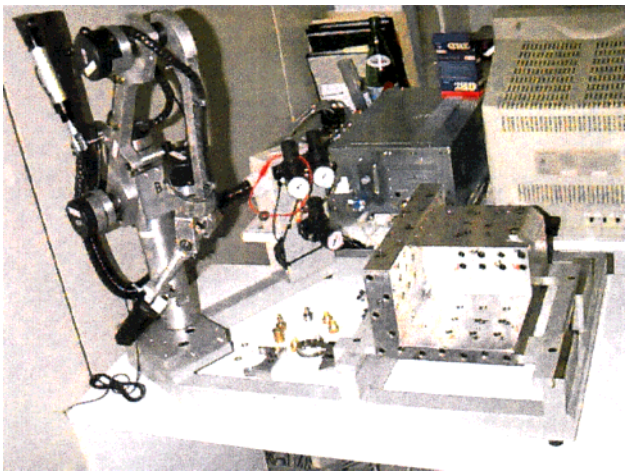

Figure 8. Measuring setup. [Color figure can be viewed in the online issue, which is available at www.interscience.wiley.com.]

The calibration procedure was performed as follows.

A total of 81 poses were collected (we call these data the *complete set*). The complete set was divided into two subsets: the *calibration set* and the *control set*. The calibration set was used as input for the program that evaluates the geometric parameters. The control set was used to verify the quality of the calibration.

In order to investigate the algorithm convergence, all the mathematical procedures were repeated three times using different sizes of the calibration and the control set:

a. 40 calibration poses, 41 control poses;
b. 60 calibration poses, 21 control poses;
c. 81 calibration poses.

To verify the quality of the calibration, for each of the 81 poses we evaluated the distance between the known gripper positions with those estimated using the measured joint rotations and the evaluated structural parameter errors (Eq. (11)). We call

these distance residual errors. The accuracy of the robot in the poses of the different subsets before calibration was estimated with the same procedure but using the nominal values of the geometrical parameters. The results are presented in Table I, which contains the average residual, its maximum value, and the standard deviation. Considering the complete set, the average position error before calibration procedure was about 4.702 mm with a standard deviation of 1.822 mm and 8.082 mm as maximum value. The values contained in the table are consistent with E_{op}, E_{it}, and E_{ka} defined in Section 3.4.

Table II presents the achieved accuracy after the calibration process performed using the three algorithms and different number of poses. For each case we give the average position errors (E_{op}, E_{it}, E_{ka}), their standard deviations, and the maximum error.

The column labelled with ''time'' represents the time necessary to process the data with a PC Pentium 100 MHz, highlighting the different efficiencies of the algorithms. The computing time included load data, parameter estimation, and save results.

A comparison of the residual error between the calibration, the control, and the complete sets gives good information about the final results. As obvious the residuals in the control set are generally worse than those in the calibration set; the residuals of the complete set are in the middle of the two. However, the differences are small, assuring that the number of the considered poses was sufficient to calibrate the robot in the considered working volume. This conclusion is supported by the fact that the results do not vary very much when increasing the calibration set from 40 to 81 poses.

The results prove the effectiveness of all the three algorithms, which reduce the gripper pose error to about 1/8 of the initial value. However, differences were present among them.

Amoeba performed the best parameter estimation, reducing the residual errors to a minimum (nearly half of *linear*); however, it was clearly much slower (about 50 times more than *linear*), requiring several minutes versus few seconds. The *kalman* algorithm behaved better than *linear*. The former was a little slower than *linear* but produced better results (close to that of *amoeba*). However, *kalman* performances degrade if the covariance matrices are initialized with unsuitable values. Moreover an analysis of the final covariance matrix **P** gives an idea of the final uncertainties of the parameter esti-

Table I. Position errors (residual) before calibration procedure.

	Calibration set [mm]				Control set [mm]			Complete set [mm]		
	Poses	average	s. dev.	max	average	s. dev.	max	average	s. dev.	max
a	40	4.789	1.784	8.082	4.616	1.854	7.572	4.702	1.822	8.082
b	60	4.692	1.785	7.574	4.732	1.921	8.082	4.702	1.822	8.082
c	81	4.702	1.822	8.082	—	—	—	4.702	1.822	8.082

Table II. Comparison between calibration algorithms: residual error (25 parameters).

		Calibration set [mm]				Control set [mm]			Complete set [mm]		
Algorithm	Time	Poses	average	s. dev.	max.	average	s. dev.	max	average	s. dev.	max
Amoeba	07′ 33″	40	0.310	0.196	0.894	0.301	0.178	0.775	0.305	0.187	0.865
	05′ 53″	60	0.399	0.261	1.127	0.461	0.192	0.828	0.415	0.246	1.117
	11′ 02″	81	0.316	0.249	1.069	—	—	—	0.316	0.249	1.069
Kalman	00′ 17″	40	0.252	0.150	0.588	0.247	0.166	0.775	0.249	0.159	0.775
	00′ 26″	60	0.247	0.156	0.849	0.290	0.176	0.888	0.258	0.163	0.888
	00′ 34″	81	0.247	0.158	0.720	—	—	—	0.247	0.158	0.720
Linear	00′ 06″	40	0.820	0.466	2.159	0.726	0.385	1.799	0.773	0.430	2.159
	00′ 08″	60	0.434	0.245	1.123	0.529	0.254	1.229	0.459	0.251	1.229
	00′ 13″	81	0.632	0.328	1.700	—	—	—	0.632	0.328	1.700

mation.[3] For the linear term the square root of the diagonal elements of **P** resulted in the range 0.002−0.029 mm, while for angles the range was 0.024−0.112 mrad.

Similar information could be possibly obtained also with the other methodologies, but that would require extra analysis that, on the contrary, is intrinsic in *kalman*.

The considered kinematics model of the robot is CPC and minimum. However, the robot is designed to operate only in a subset of its theoretical working area where it is also calibrated. In this case some of the robot parameters that theoretically are necessary could possibly be indistinguishable to others, because they produce almost the same gripper pose error in the considered working subspace. This fact can potentially reduce the effectiveness of the calibration algorithms, which sometimes work poorly with redundant parameters especially with actual data where noise is present. The term ''redundant parameters'' is used here to denote those parameters whose value cannot univocally be evaluated using the available measures. Moreover some parameters may be nonsensitive to gripper accuracy. Removing these parameters may facilitate calibration at times.

To investigate this subject, we decided to try the robot calibration, estimating just a reduced set of the parameter errors. The aim of this action was also the selection of parameters that have more influence on the gripper error of the individual robot under calibration.

We remember that complete convergence of all parameters is not necessary for a robot to be accurate within the calibrated area. However, if the robot is operated out of the calibrated area, the accuracy will depend on how well each parameter has converged. The presented methodologies calculate a robot model which best fits the measured data and which is not necessarily the correct model.

We empirically selected the parameters that we consider more important for the robot accuracy. The choice of the parameters was based on a visual inspection of the robot structure. This subset (called the *reduced set*) contains the robot base position and orientation, the joint offsets, and the link lengths; only 14 out of the 25 parameters were initially considered:

$$\Delta \mathbf{L}^* = [\Delta X_0 \quad \Delta Y_0 \quad \delta\chi_0 \quad \delta\psi_0 \quad \delta\vartheta_1 \quad \Delta d_1 \quad \delta\vartheta_2 \quad \Delta a_2 \quad \delta\vartheta_3 \quad \delta\vartheta_4 \quad \Delta d_4 \quad \delta\vartheta_5 \quad \Delta d_5 \quad \Delta Z_p]^T \tag{19}$$

For the other parameters the nominal values were assumed. The algorithms supplied an estimation of the structural parameters $\mathbf{L}^*$. These values were utilized to predict the poses of the gripper used during the measuring session. The differences between the forced and the predicted pose positions are shown in Table III, with the same convention used for Tables I and II.

The results are not very different from those obtained with the complete set of 25 parameters. In some cases they are even better. This possibly means that some ''redundancy'' was present. As a final test we designed an improved calibration program which is able to decide which parameters should be taken into account. At this point of the analysis we were interested in an easy programmable procedure based on the available software, leaving efficiency and other points to future research.

Table III. Comparison between calibration algorithms: residual error (reduced set of 14 parameters).

		Calibration set [mm]				Control set [mm]			Complete set [mm]		
Algorithm	Time	Poses	average	s. dev.	max	average	s. dev.	max	average	s. dev.	max
	02′ 11″	40	0.586	0.195	0.921	0.538	0.221	0.963	0.561	0.210	0.963
Amoeba	03′ 52″	60	0.445	0.195	1.122	0.528	0.212	1.208	0.467	0.203	1.208
	07′ 38″	81	0.294	0.189	0.926	—	—	—	0.294	0.189	0.926
	00′ 07″	40	0.341	0.169	0.858	0.315	0.143	0.775	0.328	0.157	0.858
Kalman	00′ 10″	60	0.320	0.167	0.860	0.356	0.180	0.858	0.330	0.171	0.860
	00′ 14″	81	0.319	0.167	0.846	—	—	—	0.319	0.167	0.846
	00′ 03″	40	0.711	0.214	1.256	0.669	0.214	1.129	0.690	0.215	1.254
Linear	00′ 06″	60	0.691	0.271	1.462	0.784	0.258	1.289	0.715	0.270	1.463
	00′ 07″	81	0.680	0.266	1.485	—	—	—	0.680	0.266	1.485

The program works in this way. Initially the program performs the calibration using the reduced set of parameters $\Delta\mathbf{L}^*$ and the corresponding residual error E^* is evaluated. We indicate the number of parameters in the completed as n_c, while only n_r of them are present in the reduced set. Then the calibration process is repeated $n_c - n_r$ times considering at each time the reduced set plus one of the other additional parameters. For each of these estimations a new value of E_i^* is evaluated. The parameter which generates the lower value of E_i^* is selected. If E_i^* is significantly lower than E^*, the ith parameter is added to the reduced set and the estimation procedure is repeated from the beginning.

The iterative process terminates when the inclusion of a new parameter improves the residual error less than 5%.

Results obtained with this procedure are presented in Table IV. Table V shows the parameters that have been added in the different trials by the different algorithms; figures indicate the order of insertion.

The parameters which seem most important are Δa_1, Δa_3, and $\delta\alpha_3$ which are selected more frequently and in the first iterations.

A theoretical perfect estimation of uncorrelated parameters would result in a diagonal covariance matrix $\mathbf{P}$ of *kalman*. An analysis of the value of the extra diagonal elements suggested a possible correlation between the following parameters, creating four groups:

$$\psi_0 \Leftrightarrow \vartheta_2 \qquad \vartheta_1 \Leftrightarrow \psi_2 \Leftrightarrow d_3$$
$$\vartheta_5 \Leftrightarrow a_5 \qquad d_5 \Leftrightarrow \alpha_5$$

It is interesting to see that the selection algorithms tend not to insert all the parameters of the same group, supporting the hypothesis of the presence of a certain degree of redundancy.

Table IV. Comparison between calibration algorithms: residual error (reduced set plus automatically selected parameters).

		Calibration set [mm]				Control set [mm]			Complete set [mm]		
Algorithm	Time	Poses	average	s. dev.	max	average	s. dev.	max	average	s. dev.	max
	1h 09′	40	0.238	0.175	0.693	0.240	0.153	0.722	0.239	0.164	0.722
Amoeba	1h 49′	60	0.209	0.183	0.939	0.250	0.207	0.977	0.219	0.190	0.977
	1h 44′	81	0.232	0.182	0.891	—	—	—	0.232	0.182	0.891
	07′ 18″	40	0.255	0.140	0.569	0.256	0.151	0.788	0.255	0.146	0.788
Kalman	15′ 31″	60	0.243	0.153	0.791	0.287	0.171	0.874	0.254	0.159	0.874
	22′ 27″	81	0.242	0.153	0.695	—	—	—	0.242	0.153	0.695
	00′ 52″	40	0.711	0.214	1.256	0.669	0.214	1.129	0.690	0.215	1.256
Linear	03′ 00″	60	0.469	0.185	0.896	0.536	0.183	1.022	0.487	0.187	1.022
	10′ 23″	81	0.409	0.185	0.991	—	—	—	0.409	0.185	0.991

Table V. Parameters automatically added to the reduced set $\mathbf{L}^*$.

		Added parameters										
Algorithm	Poses	Δa_1	$\delta\alpha_1$	$\delta\alpha_2$	$\delta\psi_2$	Δd_3	Δa_3	$\delta\alpha_3$	Δa_4	$\delta\alpha_4$	Δa_5	$\delta\alpha_5$
	40	2					3	1				
Amoeba	60	3		7	5		2	1	4			6
	81						2	1				
	40	4		3			2	1				
Kalman	60	3		5			2	1	6	4		7
	81	6		3			2	1	5	4	8	7
	40											
Linear	60					2		1				
	81	5				4	2	1	7	6	3	8

Comparing Table IV with Table II it is clear that the last version of the algorithm is slower but gives the best results, producing lower residual errors. For example using the *amoeba* algorithm the average residual on the complete set is reduced from 0.3–0.4 mm to about 0.2 mm. This means that at least for this experimental setup, these calibration procedures work better if a suitable reduced set of parameters is selected. The proposed selection procedure proved to be reliable and useful but it could be too slow for the case of frequent use in industrial applications. This suggests a possible future improvement based on sensitivity analysis.

6. CONCLUSIONS

Procedures for the practical calibration of a measuring robot currently employed in a manufacturing environment are presented. Three algorithms have been experimented on a 5 DOF structure under a number of different situations by applying a modified pose matching procedure which proved to be efficient and reliable.

The robot has 25 kinematic parameters to be identified. A set of 40 poses was generally sufficient to reach good results.

Although all three algorithms were able to improve the robot accuracy, they exhibit different characteristics.

Referring to the achievable final accuracy, the optimization procedure *amoeba* was clearly the best. However, it proved to be much slower than *kalman* and *linear*.

Kalman gave final good results but required a tuning phase to identify the optimal value of the covariance matrices $\mathbf{R}$ and $\mathbf{P}_0$.

The algorithm called *linear* was the faster; however, the final residual error obtained by this algorithm is almost the double than the others. The *kalman* algorithm also suggests information on the redundancy in the chosen parameter set.

In an industrial setting, for all the cases in which an initial tuning of the covariance matrices can be afforded, the use of *kalman* seems the more appropriate because it is fast, exhibits essentially the same performances of *amoeba*, and gives extra information about parameter correlation and uncertainty of the final results. During the tuning phase, comparison with the results of the other methods is invaluable.

Amoeba, which is slower, can be applied when high accuracy is required.

After the tuning phase has been completed, all the three algorithms could be run and used automatically without requiring further actions by the operator. Several prototypes of the measuring robot were successfully calibrated.

The experiment shows that the adoption of a suitable subset of parameters can sometimes improve the algorithm convergence. An automatic procedure to remove the unnecessary parameters for the individual robot under calibration is also presented. Although the adopted selection procedure could be too slow for routine use, its adoption in experimental tests confirmed the usefulness of a selection algorithm to improve calibration removing redundant or nonsensitive parameters. Future improvement can possibly be obtained using sensitivity analysis.

The calibration procedure increased the robot accuracy from 8.082 mm (maximum) and 4.702 mm (average) to a maximum of 0.891 mm and an average of 0.232 mm (*amoeba*; see Tables I and IV). This is quite good remembering that the robot repeatability is about 0.268 mm.

Some of the results are based on collaborative work with CNI s.r.l. of Bologna, Italy.

REFERENCES

1. R. Caracciolo, E. Ceresole, and A. Rossi, The off-line programming of robot for assembling tasks, Proc Int Conf Mechatronics Robotics, Duisburg/Moess, Germany, 1993, pp. 433–446.
2. S. Badocco, R. Caracciolo, M. Giovagnoni, and A. Rossi, An on-line adjusting system for assembly robots, Proc 2nd Int Symp Measurement Control Robotics, 15–19 November 1992, Tsukuba, Japan.
3. A. Omodei, G. Legnani, and R. Adamini, Three methodologies for the calibration of industrial manipulators: Experimental results on a SCARA robot, J Robotic Syst 17 (2000), 219–307.
4. W. Cleary, Robot calibration, development and testing of a laser measurement system, Honours Thesis, The University of Western Australia, October 1997.
5. B.W. Mooring, Z.S. Roth, and M.R. Driels, Fundamentals of manipulator calibration, Wiley, New York, 1991.
6. J. Denavith and R.S. Hartenberg, Trans ASME J Appl Mech 22 (1955), 215–221.
7. B.P. Flannery, W.H. Press, S.A. Tuekolsky, and W.T. Vetterling, Numerical recipes in C, the art of scientific computing, Cambridge University Press, Cambridge, UK, 1992.
8. G. Legnani and J.P. Trevelyan, Static calibration of

industrial manipulators: a comparison between two methodologies, Robotics Towards 2000 27th Int Symp Industrial Robots, 6–8 October 1996, pp. 111–116.
9. G. Legnani, C. Mina, and J. Trevelyan, Static calibration of industrial manipulators: design of an optical instrumentation and application to SCARA robots, J Robotic Syst 13 (1996).
10. International Standard ISO 9283, Manipulating industrial robots: performance criteria and related test methods.
11. A. Omodei and G. Legnani, Calibration of industrial manipulator: experimental results on an actual manipulator, SIRS'98 6th Int Symp Intelligent Robotic Syst, 21–23 July 1998, Edinburgh, UK.